



Highly active catalysts for the photooxidation of organic compounds by deposition of [60] fullerene onto the MCM-41 surface: A green approach for the synthesis of fine chemicals

John Kyriakopoulos^a, Manolis D. Tzirakis^b, George D. Panagiotou^{a,c,*}, Mariza N. Alberti^b, Kostas S. Triantafyllidis^d, Sofia Giannakaki^b, Kyriakos Bourikas^c, Christos Kordulis^{a,e}, Michael Orfanopoulos^b, Alexis Lycourghiotis^a

^a Department of Chemistry, University of Patras, GR-26500 Patras, Greece

^b Department of Chemistry, University of Crete, GR-71003 Voutes, Crete, Greece

^c School of Science and Technology, Hellenic Open University, GR-26222 Patras, Greece

^d Department of Chemistry, Aristotle University of Thessaloniki, GR-54124 Thessaloniki, Greece

^e Institute of Chemical Engineering and High-Temperature Chemical Processes (FORTH/ICE-HT), GR-26500 Patras, Greece

ARTICLE INFO

Article history:

Received 3 November 2011

Received in revised form 9 December 2011

Accepted 15 December 2011

Available online 24 December 2011

Keywords:

C₆₀
Photocatalysis
Singlet oxygen
Photooxidation
Supported catalysts
C₆₀/MCM-41

ABSTRACT

A series of C₆₀ catalysts supported on MCM-41 was prepared in the context of developing a highly active heterogeneous catalytic system for the singlet oxygen-mediated oxidation of organic substrates. Successive incipient wetness impregnation was used for preparing 3, 6, 9 and 12 wt.% C₆₀ onto MCM-41 surface. N₂ adsorption, FT-IR, XRD, HR-TEM, DRS and TGA, have been used to characterize the photocatalysts.

It was found that C₆₀ is highly dispersed (especially in the 3 and 6 wt.% C₆₀ catalysts) within the mesopores or on the external surface of MCM-41, as clusters or crystallites/aggregates of very small size and presumably in the form of atomic layers. The mesoporous structure and characteristics (surface area, mesopore size and volume) of MCM-41 remain almost intact upon deposition of C₆₀ on its surface.

The photocatalytic activity was assessed in the photocatalytic oxidation of olefins via the singlet oxygen ene reaction by studying the photooxygenation of 2-methyl-2-heptene as a probe reaction. The catalytic tests were carried out at 0–5 °C in CH₃CN under oxygen atmosphere and using a 300 W xenon lamp as the light source. To investigate further the potential applications of our catalysts we examined various types of photooxidations including the [4 + 2] or [2 + 2] cycloaddition, the heteroatom oxidation with sulfur or phosphorus containing compounds and the oxidation of phenols.

The heterogeneous photocatalysts obtained were proved to be very active exhibiting higher substrate conversion, TON and TOF values, compared to those of the unsupported (solid) C₆₀ and the corresponding photocatalysts supported on silica or γ-alumina. This was mainly attributed to the better dispersion of C₆₀ on the MCM-41. The conversion achieved over the catalysts increases with the amount of the supported C₆₀ up to a value of 6 wt.% and then it decreases whereas the TON and TOF values decrease monotonically as the amount of the supported C₆₀ increases following the increase in the size of the supported C₆₀ crystallites/aggregates. Shadow effects were not observed under our experimental conditions.

© 2011 Elsevier B.V. All rights reserved.

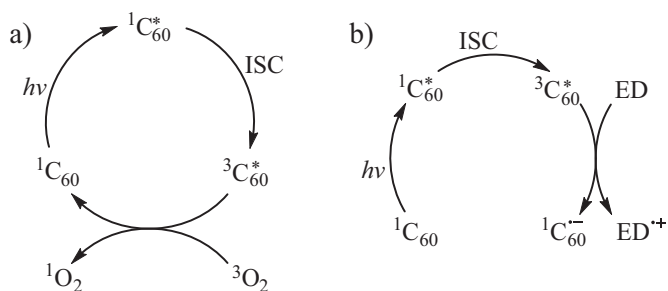
1. Introduction

Since 1921, organic syntheses have provided the chemistry community with detailed, reliable, and carefully validated procedures for the synthesis of organic compounds. Oxidation reactions possess a major role in organic synthesis. In recent years, there has been a continuing widespread interest in the photooxidation via singlet oxygen (¹O₂). Singlet oxygen (¹O₂) is the common name

used for the diamagnetic first excited state of triplet ground state oxygen (³O₂ or molecular oxygen). Because of differences in their electron shells, singlet and triplet oxygen differ in their chemical properties and reactivity. ¹O₂ is important in many diverse fields, ranging from atmospheric chemistry and materials science to biology and medicine [1,2]. Thus, singlet oxygen stays at the forefront of research because of its unique reactivity as a synthetic reagent for the synthesis of fine chemicals [3–5], as an intermediate in oxygenation reactions of polymers [6–9], in the treatment of wastewater, as a non-radical reactive oxygen species (ROS) which is closely related to tissue damages and some diseases in a range of biologically pertinent systems [10–12], including photodynamic applications such as blood sterilization, sunlight-activated

* Corresponding author at: Department of Chemistry, University of Patras, GR-26500, Patras, Greece.

E-mail address: gpanagiotou@chemistry.upatras.gr (G.D. Panagiotou).



Scheme 1. Photochemical pathways of C_{60} upon light excitation: (a) energy-transfer, and (b) electron-transfer.

herbicides and insecticides, as well as photodynamic therapy (PDT) of cancer [2,13].

Literature provides many accounts of the use of 1O_2 as a reagent in organic synthesis [1–5,14–17]. These reports reflect the fact that singlet oxygen has served as an important preparative tool in the synthesis of many natural products and other compounds of special interest. Among the various types of 1O_2 reactions, the so-called ene or Schenck reaction [18] has inevitably drawn the most extensive either experimental or theoretical attention [19,20]. The hydroperoxide formed in the 1O_2 ene reaction is usually immediately reduced to the corresponding allylic alcohol. This route is a unique way to functionalize in one step an unsaturated hydrocarbon and prepare allylic alcohols that cannot be prepared easily via other routes. Allylic alcohol derivatives are valuable products or key intermediates in the synthesis of fine chemicals.

Singlet oxygen can be generated in a photosensitized process by energy transfer from dye molecules such as xanthene dyes, porphyrins (i.e. phthalocyanines), phenothiazines (i.e. Methylene Blue) fluoresceins (i.e. Rose Bengal) and fullerenes, or by chemical processes such as spontaneous decomposition of hydrogen trioxide in water or the reaction of hydrogen peroxide with hypochlorite [3,4,21–26]. Sensitized photooxidation may be considered as a “Green Chemistry” process, since the light energy absorbed is usually in the visible range, the only reactant is air or oxygen and the reaction may be carried out in various media including water at room temperature and atmospheric pressure.

Conventionally, photosensitized reactions are carried out in homogeneous phase where separation of the products and recycling of the sensitizer come in conflict with the basic principles of “green chemistry”. A quite promising way to overcome this conflict is the development of a heterogeneous process that comprises the use of a solid, recyclable catalyst. Such a catalyst could be prepared by immobilizing the photosensitizer onto a large surface area of a solid carrier. In fact, further advantages are gained when sensitizers are grafted on an inert support in order to control aggregation and facilitate the separation of the photoactive compound from the other reactants and products.

[60] Fullerene is a well-established singlet oxygen sensitizer [24–28]. UV/vis light excitation of pristine C_{60} results in the formation of the lowest singlet excited state ($^1C_{60}^*$) which then undergoes rapid intersystem crossing (ISC) to a long-lived triplet excited state ($^3C_{60}^*$) [27,29,30]. In air-equilibrated solution $^3C_{60}^*$ is quenched by dioxygen through a triplet energy transfer from fullerene, thus giving rise to the highly reactive single excited state of O_2 , namely singlet oxygen (1O_2). The singlet oxygen quantum yield, Φ_Δ , for this process has been reported to be nearly 1.0 (excitation at 532 nm) [26,27]. The whole sensitization process is illustrated in Scheme 1a (type II energy-transfer pathway).

On the other hand, the excited triplet state of fullerene is an excellent electron acceptor, and the reduced fullerene triplet ($^3C_{60}^{\bullet-}$) is formed rapidly in the presence of electron donors (ED)

(type I electron-transfer pathway, Scheme 1b) [31,32]; this radical species may react further (e.g., through radical coupling with other organic radicals) [33–37].

Very recently a series of SiO_2 and $\gamma-Al_2O_3$ supported C_{60} catalysts with C_{60} content varying from 1 to 4 wt.% was prepared by using a simple or successive incipient wetness impregnation technique [38,39]. These catalysts exhibited higher conversion, turnover number and turnover frequency values in the photocatalytic oxidation of 2-methyl-2-heptene via the 1O_2 ene reaction, compared to those achieved over the unsupported (solid) C_{60} . In both SiO_2 and $\gamma-Al_2O_3$ supported series the catalyst that exhibited the best catalytic performance was the one having 3 wt.% C_{60} content. As reported in those studies, the high activity and stability as well as the retained activity in subsequent catalytic cycles, make these supported catalysts suitable for a small-scale synthesis of fine chemicals.

In the present study which is, in essence, a continuation of the aforementioned studies, we present the preparation of a new series of C_{60} catalysts supported on MCM-41 with the aim of achieving a much better catalytic performance of the active C_{60} species. MCM-41 is a high surface area mesoporous silica that is synthesized via templating, self-assembly methods [40–42]. It possesses long range ordered framework with uniform tubular mesopores. By changing the length of the backbone carbon chain of the surfactants used as mesopore templates and by carefully adjusting the synthesis conditions, the width (pore size) of the channels can be controlled to be within 2–10 nm. This feature, together with its very high surface area and mesopore volume, makes MCM-41 a quite promising support for the synthesis of heterogeneous supported photocatalysts [43–51]. In view of the above, we started from 3 wt.% C_{60} (best catalyst in SiO_2 and $\gamma-Al_2O_3$ supported series) and prepared three additional MCM-41 supported catalysts with C_{60} content of 6, 9 and 12 wt.%. The photocatalysts thus obtained were fully characterized in order to determine the nature, the size and the state of dispersion of the C_{60} phase as well as its stability against sublimation/combustion. Moreover, we explored the catalytic activity, of these catalytic systems in the 1O_2 oxidation of alkenes (type II pathway) by using the 2-methyl-2-heptene as a model substrate. The catalytic activity of the MCM-41 supported catalysts was found to be substantially higher when compared to that exhibited by either the unsupported or SiO_2 - and $\gamma-Al_2O_3$ -supported C_{60} catalysts. Finally, the catalytic performance of the novel catalytic systems was assessed in a series of diverse 1O_2 -mediated photooxidations of organic substrates, including the ene reaction, the [4+2] or [2+2] cycloaddition and the oxidation of phosphines, sulfides and phenols.

2. Experimental

2.1. Synthesis of MCM-41 mesoporous silica

The MCM-41 mesoporous silica was synthesized according to previously reported methods [52,53]. In a typical synthesis, 4.15 g cetyltrimethylammonium bromide (CTAB, Merck) were dissolved in 180 g water (double distilled water was used in all experiments) and 14.2 g aqueous ammonia solution (25% w/w, Merck) were then added to the CTAB solution for raising the pH to ~11.5–12. Then 15 g tetraethylorthosilicate (TEOS, Merck) were added slowly in this solution under moderate stirring. The molar composition of the synthesis gel was: 1 TEOS:0.158 CTAB:2.9 NH_3 :155 H_2O . The resulting suspension was further stirred for 1 h and then hydrothermally aged in a closed polypropylene (PP) bottle for 5 days at 100 °C. The produced solid was filtered, washed thoroughly with 2 L water and dried overnight at 90 °C. The final mesoporous silica sample was

received upon calcination of the dried material at 540 °C for 7 h under air atmosphere.

2.2. Preparation of the MCM-41 supported photocatalysts.

A series of C₆₀(x) supported photocatalysts was prepared by depositing C₆₀ onto the calcined MCM-41 silica. Solid C₆₀ was used. The x in the aforementioned notation denotes the C₆₀ content of the photocatalyst (%w C₆₀/w catalyst). The preparation method used was the successive dry impregnation technique. 1,2-Dichlorobenzene (MERCK, >98%) was used as solvent for the dilution of C₆₀. A heating step (180 °C for 1 h in air) was performed between two successive impregnation steps for the evaporation of the solvent. After the last impregnation step the prepared catalysts were dried at 180 °C for 4 h in air. By following this protocol, four catalysts were prepared having a C₆₀ content of 3, 6, 9 and 12 wt.%, respectively. Table 1 compiles the number of the impregnation steps needed for the preparation of the C₆₀ photocatalysts as well as the total amount of C₆₀ deposited onto the MCM-41 surface after every impregnation step.

2.3. Characterization of the MCM-41 supported photocatalysts.

2.3.1. N₂ adsorption-desorption measurements

The N₂ adsorption-desorption measurements were conducted at –196 °C on a Tristar 3000 porosimeter (Micromeritics). The samples were outgassed prior to analysis at 150 °C overnight, under 1 × 10^{–9} Torr vacuum. The specific surface area (SSA) of the parent calcined MCM-41 and the prepared photocatalysts was determined by the multi-point BET method by applying the BET equation in the P/P₀ range of ca. 0.05 to 0.25, the pore size distribution by the BJH analysis of the adsorption data, and the total pore volume from the N₂ uptake at P/P₀ = 0.99.

2.3.2. Diffuse reflectance spectroscopy (DRS)

The diffuse reflectance spectra of the dried photocatalyst samples were recorded at room temperature in the range 200–800 nm using a UV-Vis spectrophotometer (Varian Cary 3) equipped with an integration sphere. MCM-41 mesoporous silica was used as reference. The powdered samples were mounted in a quartz cell. This provided a sample thickness greater than 3 mm to guarantee the “infinite” sample thickness.

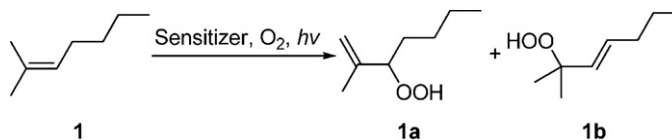
2.3.3. X-ray powder diffraction (XRD)

2.3.3.1. Range of low 2θ. The X-ray diffraction patterns (XRD) of the powdered samples in the 2θ range of 2–10° were recorded for determining the pore ordering in the mesostructure. Counts were accumulated in the range of 2–10° 2θ every 0.02° (2θ) with counting time 2 s per step. For this purpose a Siemens D-500 X-ray diffractometer with a Cu K_α radiation (40 kV, 40 mA, λ = 1.5418 Å) has been used.

2.3.3.2. Range of high 2θ. The XRD patterns of the powdered samples were also recorded in the 2θ range of 10–110° using an ENRAF NONIOUS FR 590 diffractometer. Counts were accumulated in the range of 10–110° 2θ every 0.03° (2θ) with counting time 2 s per step. A Cu K_α (λ = 1.54198 Å) radiation has been used. The generator was equipped with a curved position sensitive detector CPS120 of INEL. This was operated at 45 kV and 25 mA.

2.3.4. Fourier Transform Infrared Spectroscopy (FT-IR)

Infrared spectra were recorded in the range 400–4400 cm^{–1} with a nominal resolution of 2 cm^{–1} and averaging 10 spectra. All samples were prepared as KBr pellets and analyzed on a Perkin-Elmer 16 PC FT-IR spectrophotometer.



Scheme 2. Photooxidation of 2-methyl-2-heptene (**1**) through the ¹O₂ ene reaction.

2.3.5. Thermo gravimetric analysis (TGA)

Thermo gravimetric analysis was carried out under air in a LabsysTM TG of Setaram. For the moisture removal 10 mg of the sample was placed in an alumina crucible and was heated at 100 °C for 2 h. Then the temperature was increased from 100 to 800 °C at a heating rate 10 °C/min.

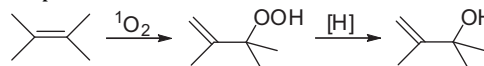
2.3.6. High Resolution-Transmission Electron Microscopy (HR-TEM)

Transmission electron microscopy was performed using a JEOL 2011 high resolution transmission electron microscope (HR-TEM) with a LaB₆ filament and an accelerating voltage of 200 kV. The microscope was also fitted with an Oxford Instruments INCAx-sight liquid nitrogen cooled EDS detector with an ultra thin window for detailed elemental analysis of the catalysts. Processing of the spectra was accomplished using the INCA Microanalysis Suite software. Samples were prepared by evaporating drops of the mesoporous catalyst-ethanol suspension after sonication onto a carbon-coated lacy film supported on a 3 mm diameter, 300 mesh copper grid.

2.4. Photocatalytic reactions

2.4.1. The model reaction

As already mentioned in the introduction, the ene reaction is invariably one of the most interesting types of reactions of ¹O₂ with organic compounds:



The allylic hydroperoxides formed initially in this reaction can be easily reduced to the corresponding allylic alcohols. These compounds have proven to be useful intermediates in the synthesis of fine chemicals.

Herein, the ene reaction of ¹O₂ with 2-methyl-2-heptene has been chosen as the model reaction to study the photocatalytic activity of the prepared catalysts. The products of this reaction are the corresponding allylic hydroperoxides **1a** and **1b** (Scheme 2).

The model reaction (Scheme 2) was carried out in 4 mL glass vial sealed with a Teflon-coated silicone septum. The reaction solution (CH₃CN, 1 mL) contained 0.03 M of 2-methyl-2-heptene, 3.6 mg of MCM-41 supported C₆₀ catalyst, and 5 μL *n*-nonane as internal standard. The corresponding unsupported C₆₀ was also evaluated under the same conditions, for comparison purposes. In this case the concentration of C₆₀ in the reaction mixture was 3 × 10^{–4} M. The reaction mixture was irradiated under a constant stream of molecular oxygen at 0–5 °C. A Cermex 300 W Xenon lamp (LX300F, ILC technology, with UV-filter output that covers a broad spectral range 390–770 nm) was used as the light source. The insoluble catalyst was kept in suspension by vigorous magnetic stirring. During irradiation aliquots of the reaction mixture were pooled out, the solid materials were filtered-off, Ph₃P was added (to reduce the allylic hydroperoxides to the corresponding alcohols) and the resulting sample was left at room temperature for 20 min. GC and/or GC-MS analysis was used to monitor the reaction over time. The % conversion values reported are the average of three measurements obtained from three separate experiments performed for each catalyst. The molar ratio **1a** and **1b** was determined by ¹H NMR spectroscopy.

Table 1Number of impregnation steps needed for the preparation of the catalysts and amount of the deposited C₆₀.

Catalyst	Amount of C ₆₀ deposited onto MCM-41 (wt.%)						
	1	2	3	4	5	6	7
C ₆₀ (3)	1.96	3.00					
C ₆₀ (6)	1.96	3.85	6.00				
C ₆₀ (9)	1.96	3.85	5.67	7.41	9.00		
C ₆₀ (12)	1.96	3.85	5.67	7.41	9.09	10.7	12.0

The turnover number (TON) was calculated by dividing the concentration of products **1a** and **1b** (mol of products) with the amount of the supported C₆₀ (mol of C₆₀). The turnover frequency (TOF) was calculated by dividing TON with the irradiation time (s).

2.4.2. Solvents and reagents

Commercially available solvents or reagents were used as received without further purification. Unless otherwise noted acetonitrile HPLC-grade was used as the reaction solvent. Diethylether was distilled from Na under N₂ prior to use.

2-Methyl-2-heptene was prepared as previously reported [38,39] in 50% yield by Wittig reaction of isopropyltriphenylphosphorane with pentanal and purified by fractional vacuum distillation. Spectral data (¹H NMR, ¹³C NMR, MS) are consistent with previous reports on this compound [38,39].

The photocatalytic activity of the prepared MCM-41 supported catalysts was further explored in various ¹O₂-mediated reactions. The non-commercially available substrates used in these studies have been prepared according to the experimental procedures shown below.

1,1-Diphenylethylene was prepared as previously reported [54] in 69% yield by a Grignard reaction between benzophenone and methylmagnesium bromide followed by dehydration in the presence of a catalytic amount of *p*-toluenesulfonic acid. 1,1-Diphenylethylene was purified by silica gel chromatography. Spectral data (¹H NMR, ¹³C NMR, MS) are consistent with the previous report on this compound [54].

9-Methylene-9H-fluorene was prepared by a Grignard reaction between 9H-fluoren-9-one and methylmagnesium iodide followed by dehydration in the presence of a catalytic amount of *p*-toluenesulfonic acid. These reactions are described in detail below.

9-Methyl-9H-fluoren-9-ol: This compound was prepared by a Grignard reaction between 9H-fluoren-9-one and methylmagnesium iodide. To a solution of Mg (0.97 g, 40 mmol) and catalytic amount of I₂ in 20 mL dry Et₂O was added dropwise methyl iodide (1.25 mL, 20 mmol) in 20 mL dry Et₂O. The mixture was refluxed for 1 h. Subsequently, the solution was cooled to 0 °C and 9H-fluoren-9-one (3.39 g, 18.8 mmol) was added dropwise. After 30 min the mixture was allowed to warm to room temperature where it was stirred for 2–3 h. The solution was worked up with NH₄Cl solution and extracted three times with Et₂O. The organic layers were combined, dried (MgSO₄), filtered and concentrated to afford 9-methyl-9H-fluoren-9-ol that was used without any further purification. Overall yield 86%. ¹H NMR (CDCl₃, 300 MHz) δ 7.60 (d, 2H, *J* = 7.0 Hz), 7.51 (d, 2H, *J* = 7.0 Hz), 7.32 (m, 4H), 2.18 (s, 1H, OH), 1.69 (s, 3H) ppm; ¹³C NMR (75 MHz, CDCl₃) δ 150.0, 138.9, 129.0, 128.1, 123.4, 120.1, 79.6, 26.2 ppm; MS *m/z* = 181.0 (100, *m/z* = 181.0).

9-Methylene-9H-fluorene: A solution of 9-methyl-9H-fluoren-9-ol (3.17 g, 16.16 mmol) in benzene (80 mL) containing catalytic amount of *p*-toluenesulfonic acid was heated at 70 °C for 2–3 h. The solution was dried (MgSO₄), filtered and then concentrated. The crude product was chromatographed on silica gel (hexanes/EtOAc = 9:1) to give 9-methylene-9H-fluorene as a yellow solid in 17% overall yield. ¹H NMR (CDCl₃, 300 MHz) δ 7.76 (m, 4H), 7.40 (m, 4H), 6.12 (s, 2H) ppm; ¹³C NMR (75 MHz, CDCl₃) δ 140.2,

138.1, 128.8, 127.1, 121.1, 120.0, 107.8 ppm; MS *m/z* = 178.1 (100, *m/z* = 178.1).

2.4.3. Analytical and chromatographic techniques

¹H NMR and ¹³C NMR spectra were recorded on Bruker AMX-500 MHz (125 MHz for ¹³C) and DPX-300 MHz (75 MHz for ¹³C) spectrometers, in CDCl₃. Chemical shifts are reported in ppm relative to TMS using the residual solvent signals at 7.26 and 77.16 ppm as internal references for the ¹H and ¹³C spectra, respectively. GC-MS analysis was performed on a Shimadzu GC MS-QP5050A apparatus equipped with a Supelco capillary column (MDN-5, 30m × 0.25 mm × 0.25 μm film thickness) and CI mass detector (5971A MS). Gas chromatographic analyses was carried out using a Hewlett Packard 5890 series II instrument, equipped with HP silica fused capillary column (20% permethylated β-cyclodextrin, 30m × 0.25 mm I.D. × 0.25 μm film thickness). UV–vis spectra were recorded on a Shimadzu MultiSpec-1501 UV/Visible spectrometer.

Thin Layer Chromatography (TLC) was carried out on SiO₂ (silica gel F254) and flash column chromatography was carried out on SiO₂ (silica gel 60, SDS, 230–400 mesh ASTM).

3. Results and discussion

3.1. Physicochemical characteristics of the prepared photocatalysts

3.1.1. Verification of C₆₀ loading onto MCM-41

Fig. 1 illustrates the FT-IR spectra recorded for the MCM-41, the prepared catalysts and the solid C₆₀. By comparing the spectra of C₆₀ (see inset) with those of the supported catalysts, it becomes obvious that the peaks at 526 and 575 cm^{−1} in the spectra of C₆₀(*x*) derivatives are due to the successful incorporation of C₆₀ in MCM-41. As expected, these two peaks are more intense in the samples with the higher amount of C₆₀. Moreover, no shift is observed in the

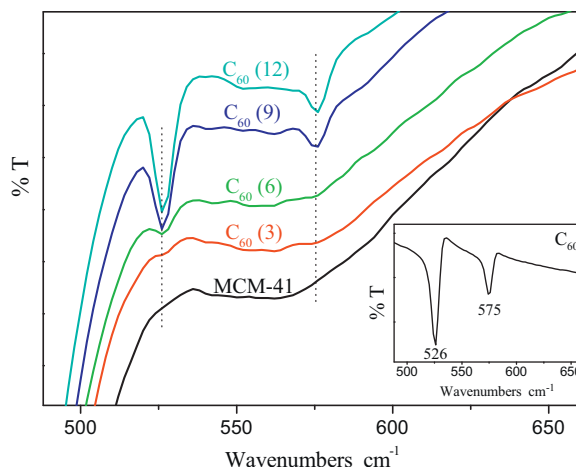


Fig. 1. FT-IR spectra recorded in the range 500–650 cm^{−1} for the support (after impregnation with 1,2-dichlorobenzene and heating at 180 °C for 4 h) and the prepared catalysts. Inset: FT-IR spectra recorded in the range 500–650 cm^{−1} for the solid C₆₀.

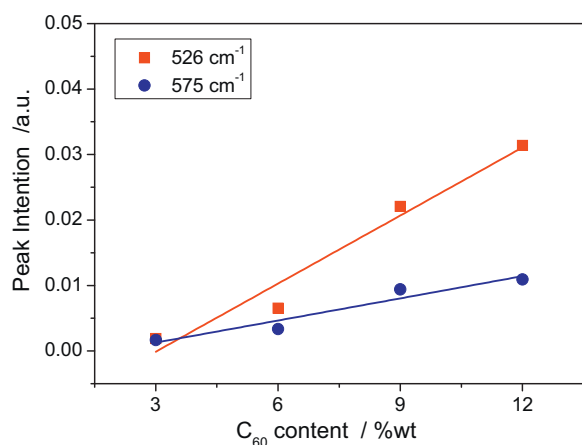


Fig. 2. Dependence of the intensity of the C₆₀ peaks at 526 cm⁻¹ and 575 cm⁻¹ on the C₆₀ content in the studied photocatalysts.

absorption bands which indicates that the nature of the C₆₀ species has not been changed upon the deposition of C₆₀ on the MCM-41 surface or due to possible interactions with the silica during heating of the impregnated samples. This conclusion is further corroborated by the linearity observed in Fig. 2 between the intensity of the aforementioned peaks and the C₆₀ content in the photocatalysts.

3.1.2. Porosity, structure and morphology of the supported C₆₀ mesoporous catalysts

The pore size distribution of the parent MCM-41 silica support and the prepared photocatalysts are illustrated in Fig. 3. Table 1 compiles the values of the specific surface area, pore size and total pore volume of the support, C₆₀ and the prepared photocatalysts.

The N₂ adsorption-desorption measurements has shown that the MCM-41 comprises uniform mesopores having a diameter of about 2.7 nm (Fig. 3, Table 2). The deposition of the C₆₀ on the MCM-41 surface does not change the pore size of the support. On the other hand, a small decrease is observed in the SSA and the pore volume of the studied photocatalysts. The variation of the SSA of the MCM-41 support (i.e. estimated on the basis of the silica portion of each catalyst) with C₆₀ loading is presented in Fig. 4. It is evident that a greater reduction in the SSA of the support, which however does not exceed 5%, is observed for the photocatalysts having 9 and 12 wt.% C₆₀, possibly due to a limited pore blocking at these high carbon loadings. In contrast, only a slight decrease in the SSA of the support is caused by the deposition of 3 and 6 wt.% C₆₀.

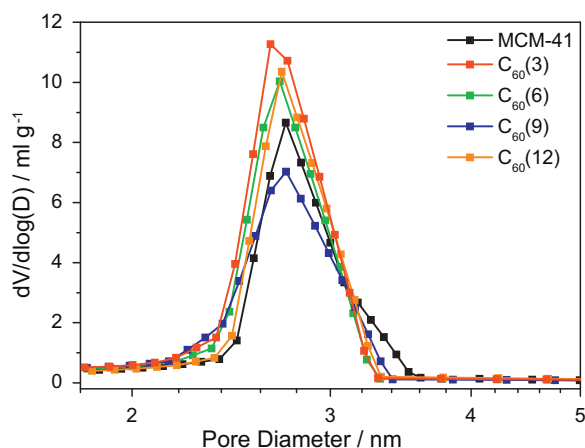


Fig. 3. Pore size distribution [dV/dlog(D)] of parent MCM-41 and the prepared supported C₆₀(x) photocatalysts.

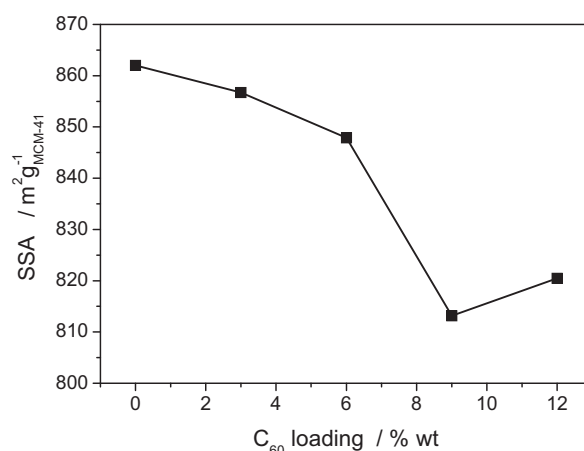


Fig. 4. Decrease in the SSA of MCM-41 caused upon deposition of different amounts of C₆₀.

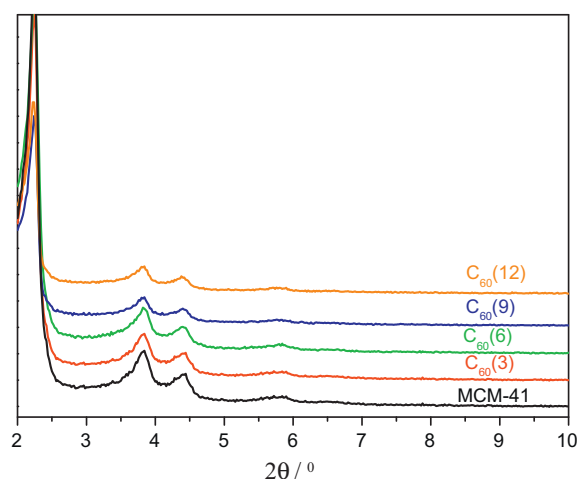


Fig. 5. XRD patterns recorded in the 2θ range of 2–10° for the support and the prepared catalysts.

The XRD results are presented in Figs. 5 and 6. The XRD patterns recorded in the 2θ range of 2–10° for the MCM-41 support and all the studied photocatalysts (Fig. 5) seem to be identical. Indeed, this confirms the above claim that the deposition of C₆₀ on the MCM-41

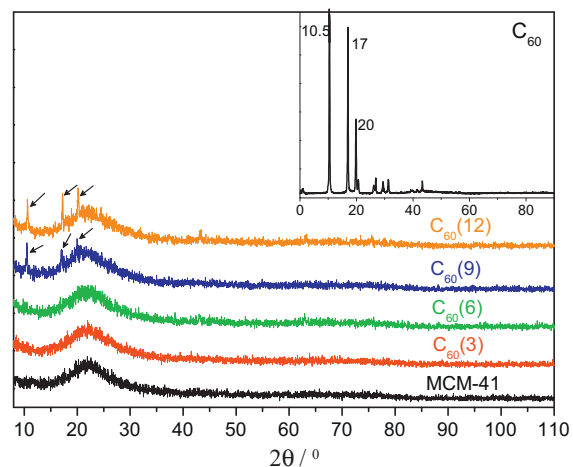


Fig. 6. XRD patterns recorded in the 2θ range of 10–110° for the support, the prepared catalysts and solid C₆₀ (inset).

Table 2Porosity characteristics of C₆₀, MCM-41 and the prepared photocatalysts.

Sample	SSA/catalyst (m ² g ⁻¹)	SSA/support (m ² g ⁻¹ _{MCM-41})	Total pore volume (cm ³ g ⁻¹)	Pore diameter (nm)
C ₆₀	<10	–	<0.01	–
MCM-41	862	862	0.82	2.72
C ₆₀ (3)	831	857	0.78	2.68
C ₆₀ (6)	797	848	0.75	2.68
C ₆₀ (9)	740	813	0.70	2.70
C ₆₀ (12)	722	820	0.70	2.71

surface does not change or destroy the ordered mesostructure of MCM-41.

The diffraction peaks obtained for the unsupported C₆₀ (inset of Fig. 6) do not appear in the XRD patterns recorded for the photocatalysts with low C₆₀ content (3 or 6 wt.%). This corroborates the formation of C₆₀ clusters or crystallites of rather small size on the MCM-41 surface, which are not visible by XRD. In contrast, the most intense peaks of C₆₀ (at 2θ 10.5, 17 and 20) do appear in the XRD spectra of the catalysts containing 9 and 12 wt.% C₆₀. This means that when the content of C₆₀ on the support surface exceeds 6 wt.%,

C₆₀ crystallites with size bigger than ca. 3 nm begin to form on the support surface.

Fig. 7 illustrates the HR-TEM images taken for the photocatalyst having the highest amount of C₆₀. We observe that the porous structure of MCM-41 remains intact upon deposition of a relative high amount of C₆₀ on its surface. This is in accordance with the XRD findings discussed above. Although images were taken at various magnifications it was impossible to detect any carbon phase, amorphous or aggregates, on the surface of MCM-41; however, the presence of carbon all over the catalyst surface was verified by the

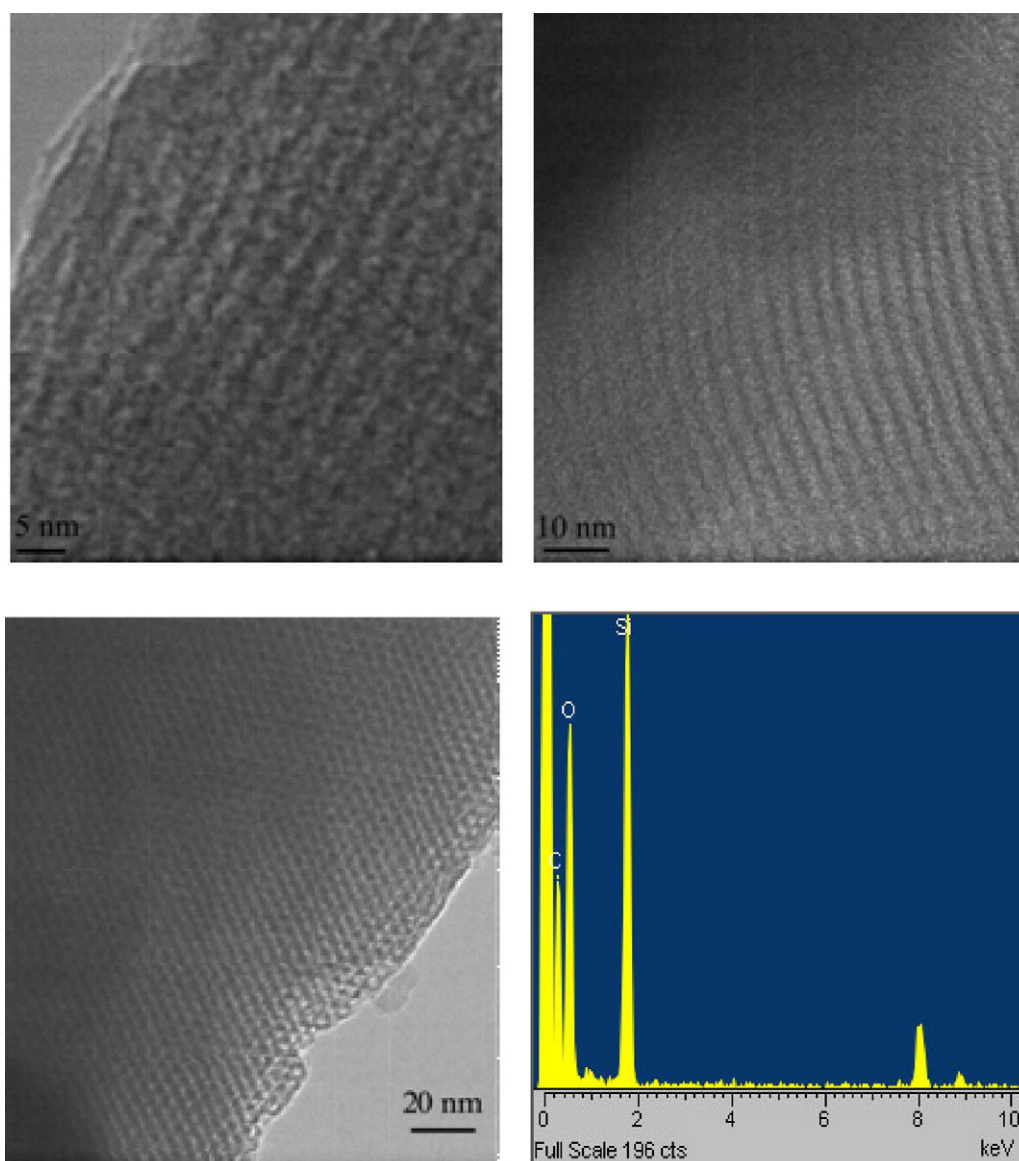


Fig. 7. High Resolution TEM images (at various magnifications) and Elemental Analysis results of the C₆₀(12) photocatalyst. The various elements detected are indicated.

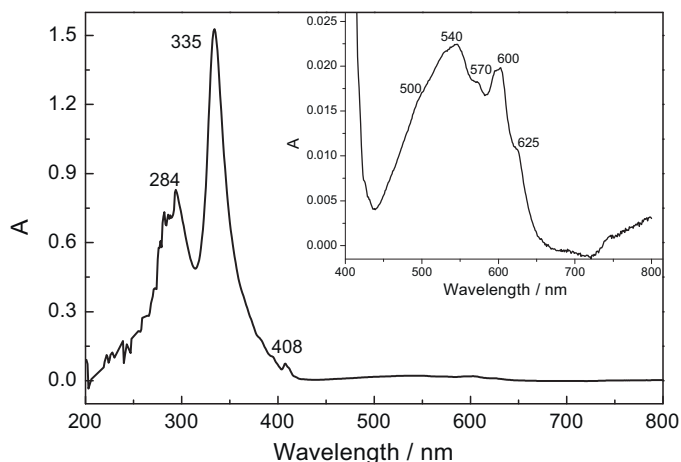


Fig. 8. Absorbance spectrum of a C_{60} solution in 1,2-dichlorobenzene recorded in the range 200–800 nm. 1,2-Dichlorobenzene was used as reference. Inset: a magnification of the spectrum in the visible region.

EDS results (Fig. 7). Identical images were also recorded for the other three photocatalysts, having lower content of C_{60} . The above results coming from the HR-TEM and XRD techniques suggest that the C_{60} is highly dispersed either on the internal surface of the pores or on the external surface of the silica particles in the form of atomic layers less than ca. 3–4 in number (assuming a C_{60} monolayer thickness of 1 nm), for all the four supported catalysts. The low intensity XRD peaks due to C_{60} observed in the XRD patterns of the 9 and 12% C_{60} supported catalysts could be attributed to the formation of some relatively larger aggregates (ca. bigger than 3 nm) which are randomly dispersed on the surface of the MCM-41 particles and cannot be easily detected by TEM investigation.

3.1.3. The dispersion of C_{60} on MCM-41 surface studied by DRS

The electronic spectrum of a C_{60} solution in 1,2-dichlorobenzene is illustrated in Fig. 8. In the UV–Vis absorption spectrum of the dissolved C_{60} two strong absorption peaks appear at 284 and 335 nm, a smaller absorption peak at 408 nm and a very weak band extended in the visible region. The magnification of the spectrum in the visible region shows that the large band (475–650 nm) is rather structured involving five peaks at about 500, 540, 570, 600 and 625 nm. The aforementioned peaks in the ultraviolet and visible region are in good agreement to those found in the literature [55–57]. The peaks at 284, 335 and 408 nm are attributed to C_{60} molecules/clusters or very small aggregates. On the other hand, the weak band in the visible region may be attributed to slightly larger C_{60} aggregates. This is corroborated by the observation that the DR spectrum of the solid (unsupported) C_{60} exhibits stronger absorption bands in the visible region rather than in ultraviolet region (Fig. 9, inset).

The DR spectra of the prepared photocatalysts recorded using MCM-41 as a reference material (its spectrum is also shown for comparison) are illustrated in Fig. 9. In all the photocatalysts examined, a wide band appears in the range 200–700 nm with eight distinct peaks at 210, 262, 340, 405, 450, 510, 625 and 680 nm. The photocatalysts with 3 and 6 wt.% C_{60} exhibit similar DR spectra. These are characterized by strong absorption bands in the UV region and a weaker absorption band in the visible region. These spectra appear to be very similar with the spectrum recorded for the C_{60} solution in 1,2-dichlorobenzene (Fig. 8) indicating the formation of C_{60} molecules/clusters or very small aggregates on the support surface. As the amount of C_{60} deposited on MCM-41 increases, the absorption band in the visible region becomes stronger. This suggests that when the C_{60} deposited on the MCM-41 surface exceeds 6 wt.%, crystallites/aggregates of relative larger size are formed.

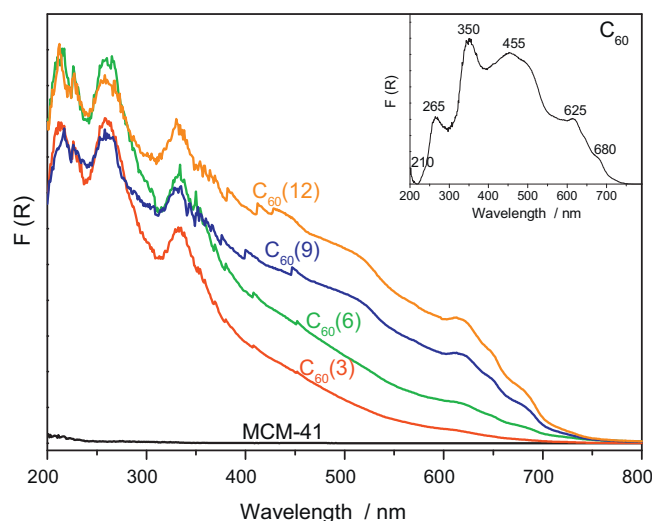


Fig. 9. DR spectra recorded in the range 200–800 nm for the support, the prepared catalysts and the solid C_{60} (inset).

The above findings are in agreement with the XRD results discussed above.

It is worth noting that the DR spectrum for the photocatalyst C_{60} (3) is quite different compared to that obtained for the C_{60}/SiO_2 photocatalyst containing the same amount of C_{60} [39]. In the latter case strong absorption peaks appear also at wavelengths higher than 400 nm which are attributed to C_{60} aggregates of medium and presumably of somewhat larger size. The above finding is attributed to the higher surface area of MCM-41 compared to that of SiO_2 . The surface area of MCM-41 is about four times larger than the surface area of silica ($226\text{ m}^2/\text{g}$), thus inducing a better dispersion of C_{60} and the formation of clusters or crystallites/aggregates of very small size.

3.1.4. Stability of the supported C_{60}

There is a critical temperature above which the solid C_{60} is sublimated/combusted in the presence of air. Therefore, in order to investigate the thermal stability of all the prepared photocatalysts we carried out TGA experiments. This technique is quite useful as it provides information about the temperature range where the photocatalysts are stable and thus can be used in various photocatalytic reactions. Fig. 10 illustrates the TGA curves recorded for all the prepared photocatalysts.

Prior to TGA, the samples were thermally treated in situ for 2 h at 100°C for the removal of the physically sorbed water on MCM-41 surface. As a result the weight loss for the parent calcined MCM-41 over the 100 – 800°C temperature range was only about 2%, mainly due to surface dehydroxylation. The sublimation/combustion of the unsupported C_{60} starts at about 500°C , leaving also a char/residue of about 15% at 800°C . The C_{60} sublimation/combustion in the photocatalysts starts at about 450°C and is completed at 600°C . This is because the formed C_{60} clusters or small crystallites on the support surface (compared with that of the unsupported C_{60}) are more easily burned compared to the bulk C_{60} . Still, however, the dispersion of C_{60} on the surface of MCM-41 did not significantly alter its stability upon sublimation/combustion.

3.2. Photocatalytic activity of the catalysts

3.2.1. The activity of the prepared photocatalysts as a function of the loading of the sensitizer

The photocatalytic activity of the above four catalytic systems, has been assessed by studying the photooxidation of

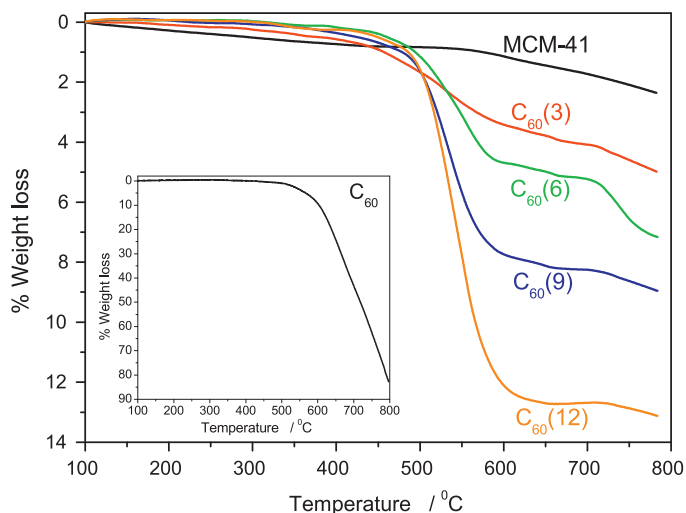


Fig. 10. TGA curves recorded in air for the prepared photocatalysts. Inset: TGA curve of the unsupported C_{60} .

2-methyl-2-heptene (**1**) as a model reaction. All the heterogeneous catalytic reactions were carried out under the same conditions, using 0.03 M of **1** and 3.6 mg of the different $C_{60}(x)$ photocatalysts studied. The kinetic curves obtained are shown in Fig. 11. In these curves the % conversion of **1** is plotted as a function of reaction time. For comparison, the corresponding reaction over the unsupported C_{60} was also evaluated (black line in Fig. 11).

In all cases the allylic hydroperoxides **1a** and **1b** were obtained in a 1:1 molar ratio. Moreover, the photooxidation of **1** in the presence of well-established 1O_2 sensitizers, such as Rose Bengal (RB) or TetraPhenyl Porphyrine (TPP) afforded **1a** and **1b** in the same ratio. This result is indicative of a 1O_2 formation as the reactive intermediate in the case of the C_{60} mediated heterogeneous photooxidation of **1**. Further experiments performed with the addition in the reaction mixture of 5 mg of 1,4-diazabicyclo[2.2.2]octane, an excellent $^3C_{60}^*$ and 1O_2 quencher, revealed an almost complete inhibition of the $C_{60}(6)$ sensitized photooxidation of **1**.

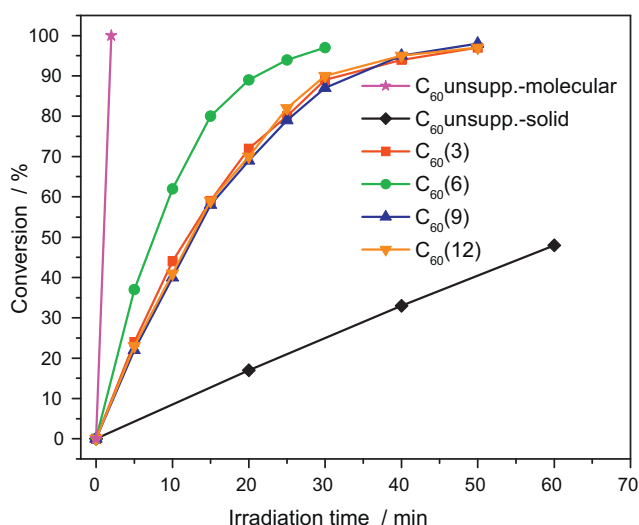


Fig. 11. Variation of the conversion of 2-methyl-2-heptene with irradiation time over the catalysts studied. The corresponding values for the unsupported-solid C_{60} and the unsupported-molecular C_{60} under homogeneous conditions were also determined for comparison purposes. In both cases the concentration of C_{60} in the reaction mixture was 3×10^{-4} M. This corresponds to that involved in the suspension of the $C_{60}(6)$ photocatalyst. The photocatalysts used are indicated.

When the model reaction was run in the presence of pure MCM-41 an insignificant oxidation was observed indicating that the MCM-41 does not interfere to the photocatalyzed reaction. Similarly, control experiments in the absence of catalyst showed no oxidation of the substrate in the presence of molecular oxygen. In addition, no oxidation products were observed when blank experiments were run in the dark. These results thus clearly provide an evidence of the crucial role played by the highly dispersed supported C_{60} clusters or crystallites in the studied photocatalytic process.

Also, it may be observed that under the conditions explored, the substrate is essentially quantitatively converted to the corresponding oxygenated products in 20–40 min of irradiation. More importantly, it may be seen that the activity of the MCM-41 supported catalysts is much higher than that obtained for the unsupported C_{60} . For example, the percentage conversions obtained after 30 min of irradiation over the $C_{60}(6)$ and C_{60} photocatalysts were found to be equal to 97% and 23%, respectively. It should be mentioned that the same amount of C_{60} is involved in both cases. Furthermore, it can be seen that the increase of the C_{60} loading from 3 to 6 wt.% leads to an increase of the photocatalytic activity of the corresponding $C_{60}(x)$ catalysts. On the other hand, the photocatalytic activity of the $C_{60}(9)$ and $C_{60}(12)$ samples did not follow the same trend exhibited a slightly lower activity than that of the $C_{60}(6)$ catalyst. Thus, the maximum catalytic activity can be obtained by using a supported photocatalyst with a C_{60} content of about 6 wt.%.

The increase in the photocatalytic activity up to 6 wt.% seems to follow approximately the increase in the C_{60} content of the photocatalyst but an inversion is observed above this content. It is important to stress that the inversion is observed in the samples, where relatively larger C_{60} crystallites are formed on the support surface. This behavior implies that the intrinsic activity is not constant but depends on the size of the supported C_{60} crystallites/aggregates. To investigate further this behavior we determined the turnover number (TON) and the turnover frequency (TOF) for the studied photocatalysts. The variation of these parameters with irradiation time is illustrated in Fig. 12(a) and (b), respectively.

It can be clearly evidenced by Figs. 12(a) and (b) that the TON and TOF values decrease with the increase of C_{60} content. Therefore, the intrinsic activity follows the opposite trend to that followed by the C_{60} loading. This could probably explain the inversion in the conversion observed above. One could attribute the decrease in the intrinsic activity with the C_{60} content to the increase of the size of the C_{60} crystallites/aggregates. This size seems to be an important factor determining the catalytic activity. In order to examine further this point we attempted to investigate the same reaction under conditions where the C_{60} is molecularly dispersed (minimum size). Thus, the above reaction catalyzed by molecular C_{60} under homogeneous conditions in either benzene or toluene has been also evaluated (Fig. 11). This homogeneous catalytic reaction was performed under similar conditions with those used in the corresponding heterogeneous reaction with the $C_{60}(6)$ catalyst. Thus, a 0.03 M solution of 2-methyl-2-heptene (**1**) in 1 mL of benzene or toluene was irradiated in the presence of 3×10^{-4} M C_{60} , at 0°C under O_2 atmosphere. As expected by virtue of the higher dispersion of C_{60} in this case (molecular dispersion), the homogeneous reaction was much faster than its heterogeneous analogue. In particular, a quantitative conversion of **1** was achieved in 2 min, instead of 25 min that had been observed in the corresponding heterogeneous reaction. The observed difference in reactivity, however, cannot be regarded as evidence of limited efficiency of the heterogeneous systems studied herein. In contrast, the present results show that the supported catalysts $C_{60}(x)$ retain the advantages of both homogeneous (i.e. very fast reaction with respect to

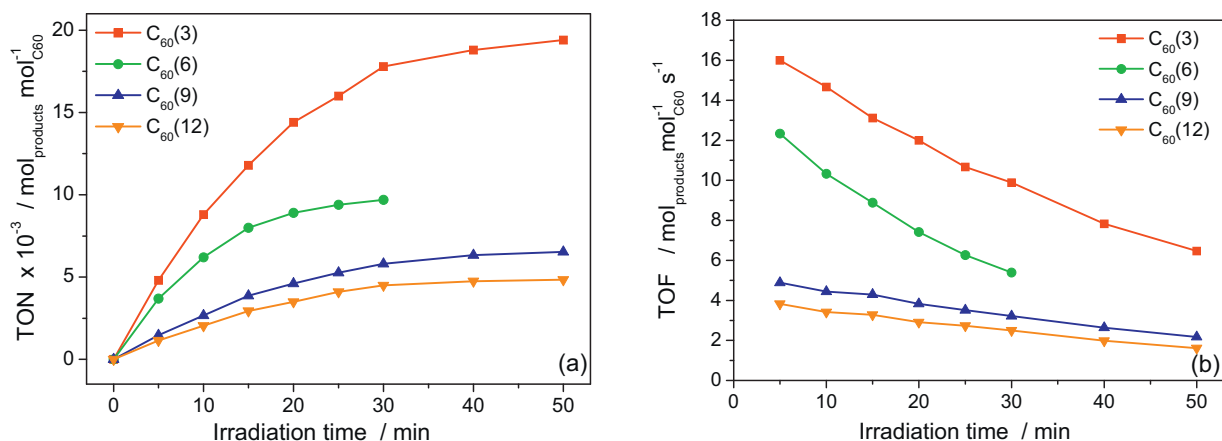


Fig. 12. The variation of (a) TON and (b) TOF with irradiation time, for the studied photocatalysts.

the unsupported, solid, C_{60}) and heterogeneous catalysis (i.e. easy removal of catalyst after reaction and reuse).

Closing this subsection it should be mentioned that a critical point is the reusability of the photocatalysts developed. Preliminary experiments done in the frame of the present work have shown that the photocatalytic activity does not change considerably at least for 2 subsequent cycles. This is further investigated in detail in a subsequent work in relation with the method of deposition of the sensitizer on the surface of the MCM-41.

3.2.2. Effect of solvent on the photocatalytic activity

To investigate the effect of the solvent in the photocatalytic behavior, the catalyst that exhibited the highest activity in acetonitrile, namely $C_{60}(6)$, was tested in the photooxidation of 2-methyl-2-heptene (**1**) in different solvents. Fig. 13 illustrates the catalytic performance of $C_{60}(6)$ in the oxidation of 2-methyl-2-heptene using acetone, hexane, ethyl acetate and acetonitrile as the reaction solvent.

All solvents seem to be suitable for the aforementioned photooxidation. The small differences observed could be related to the polarity of the solvent which would affect the solubility of C_{60} [58,59] and the life time of the singlet oxygen. In any case CH_3CN was proved to be the best solvent. The same was observed for the C_{60} supported on silica or alumina [38,39].

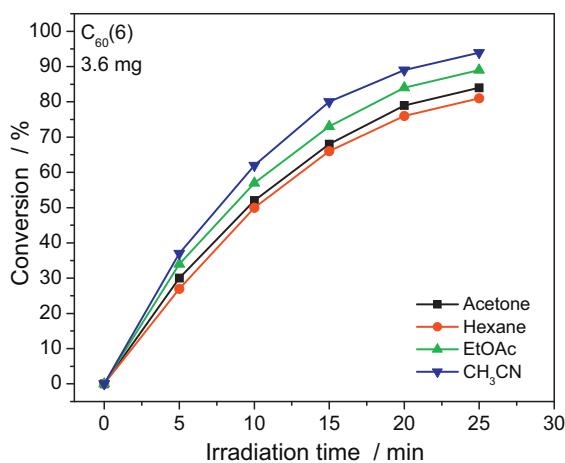


Fig. 13. Catalytic performance of $C_{60}(6)$ photocatalyst in the heterogeneous photooxidation of 2-methyl-2-heptene using different solvents. The catalyst amount in the suspension is indicated.

3.2.3. Effect of the photocatalysts amount on the photocatalytic activity: investigating shadow effects

The effect of the catalyst amount on the photocatalytic activity was then studied using five different suspensions of the $C_{60}(6)$ photocatalyst in 1 mL CH_3CN . These suspensions contained various amounts of the aforementioned catalyst and thus different concentrations of the sensitizer ranging from 1.0×10^{-4} to 6.0×10^{-4} M. All the suspensions, having 0.03 M of 2-methyl-2-heptene, were then irradiated for 30 min under continuous oxygen bubbling at $0-5^\circ\text{C}$. The results obtained are illustrated in Fig. 14.

We observe that the increase in the amount of the catalyst in the reaction mixture causes an increase in the conversion. The maximum value of the reaction conversion has not yet reached indicating the absence of shadow effects for all C_{60} concentrations studied.

3.2.4. Formal kinetic investigation

The photocatalytic behavior of the $C_{60}(x)$ photocatalysts developed was further investigated by studying the formal kinetics of the photooxidation of 2-methyl-2-heptene. Assuming a first order dependence of the reaction rate on the concentration of 2-methyl-2-heptene and taking into account that during the photocatalytic reaction the oxygen concentration in the reaction mixture

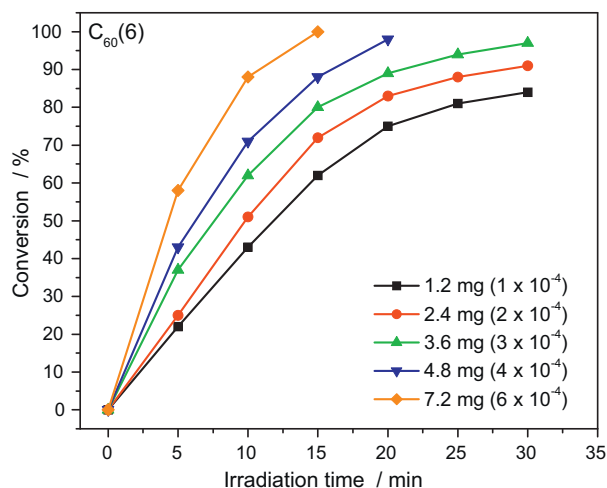


Fig. 14. Time profiles of the 2-methyl-2-heptene photooxidation catalyzed by five different suspensions of varying catalyst amount in oxygen saturated CH_3CN at $0-5^\circ\text{C}$. The catalyst amount in the suspension and C_{60} concentration (values in parentheses) are indicated.

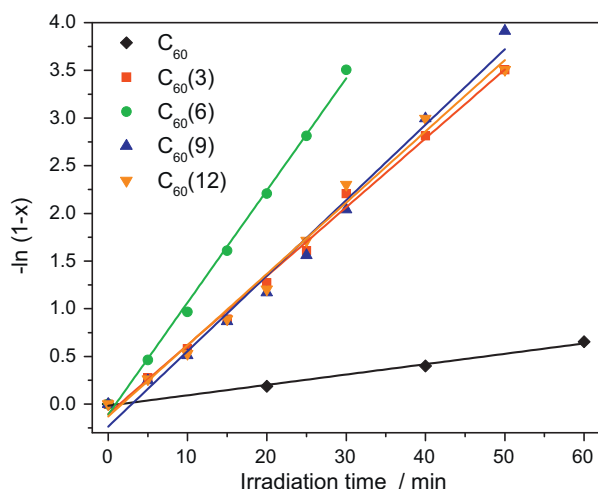


Fig. 15. Dependence of “ $-\ln(1-x)$ ” appeared in eq. (1) on “ t ” for the photooxidation of 2-methyl-2-heptene over the unsupported C_{60} and the studied photocatalysts.

remained constant, the following well known equation can be written:

$$kt = -\ln(1-x) \quad (1)$$

This equation relates the reaction time (t), the reaction rate constant (k) and the conversion of 2-methyl-2-heptene (x). Fig. 15 illustrates the variation of the “ $-\ln(1-x)$ ” with “ t ”.

It can be seen that in all cases there is good linearity between the aforementioned terms confirming that there is indeed a first order dependence of the reaction rate on the concentration of 2-methyl-2-heptene. Fig. 15 also indicates that the same kinetics is followed over the unsupported and supported C_{60} .

Table 3 compiles the values of the rate constant per gram catalyst and per mmol of the supported C_{60} . These values were easily calculated by the slope of the linear curves. As expected, the first constant values follow the same trend as the % conversion (Fig. 11) whereas the latter values follow the same trend as TOF (Fig. 12).

3.2.5. Catalytic comparison of C_{60} photocatalysts supported on various oxidic supports

The aim of this section is the direct comparison between the results obtained in our previous studies for the SiO_2 and $\gamma-Al_2O_3$ supported C_{60} photocatalysts [38,39] and our present results on the corresponding MCM-41 supported catalysts. Fig. 16 shows the variation of the conversion of 2-methyl-2-heptene with irradiation time for the catalysts supported on MCM-41 as well as for two catalysts supported on SiO_2 and $\gamma-Al_2O_3$ which exhibited the highest activity in our previous studies [38,39].

In both SiO_2 and $\gamma-Al_2O_3$ series the catalyst with 3% C_{60} exhibited the best catalytic performance. It is clear that the $C_{60}(3)$, supported on MCM-41 presents much better catalytic activity. This could be attributed to the very high SSA of the MCM-41 which favors better dispersion and thus smaller supported crystallites/aggregates of the sensitizer.

Table 3

Values of the rate constant calculated per gram of the catalyst and per mmol of the supported C_{60} .

Catalysts	k (g _{cat} min ⁻¹)	k' (mmol _{C₆₀} min ⁻¹)
$C_{60}(3)$	20.1	482
$C_{60}(6)$	32.7	392
$C_{60}(9)$	22.0	176
$C_{60}(12)$	20.8	125

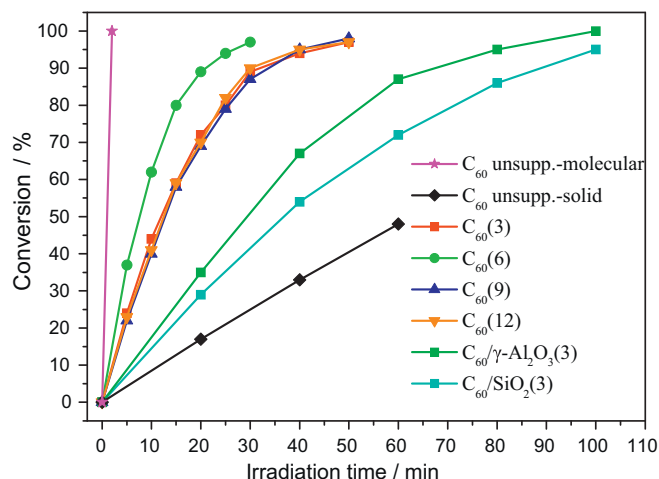


Fig. 16. Variation of the conversion of 2-methyl-2-heptene with irradiation time over the MCM-41 supported catalysts and over the two catalysts supported on SiO_2 and $\gamma-Al_2O_3$ that were the most active in the corresponding series. The corresponding values for the unsupported-solid C_{60} and the unsupported-molecular C_{60} under homogeneous conditions are also presented. The photocatalysts used are indicated. The numbers in parentheses represent the percentage amount (wt.%) of C_{60} in the catalysts.

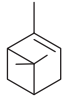
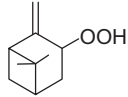
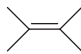
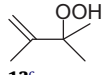
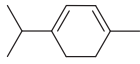
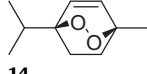
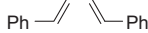
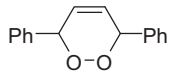
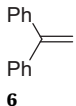
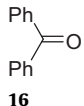
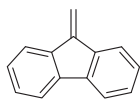
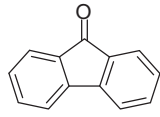
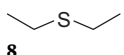
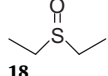
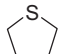
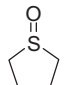
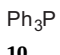
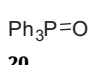
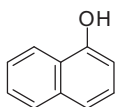
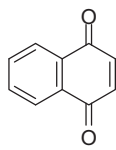
3.2.6. Heterogeneous photocatalyzed oxidation of other organic substrates 2–11

The most common 1O_2 -mediated reactions are the following: (1) the aforementioned ene reaction, (2) the [4 + 2] cycloaddition [60–62] with conjugated dienes to afford endoperoxides, (3) the [2 + 2] cycloaddition [60,63] with electron-rich alkenes to yield 1,2-dioxetanes, (4) the heteroatom oxidation with sulfur, phosphorus and nitrogen compounds as well as organometallic complexes [3] and (5) the oxidation of electron-rich aromatic compounds, such as phenols [64].

In the previous subsections, we reported on the catalytic activity of the $C_{60}(x)$ catalysts regarding the heterogeneous photooxidation of 2-methyl-2-heptene via a 1O_2 ene reaction. In this subsection we wish to further probe the potential applications of these catalysts as useful photosensitizers in various 1O_2 -mediated reactions. For this purpose, we examined the 1O_2 -mediated: (1) ene reaction of α -pinene and 2,3-dimethyl-2-butene, (2) [4 + 2] cycloadditions of α -terpinene and *trans,trans*-1,4-diphenyl-1,3-butadiene, (3) [2 + 2] cycloadditions of 1,1-diphenylethylene and 9-methylene-9H-fluorene, (4) oxidations of diethyl sulfide, tetrahydrothiophene and triphenylphosphine, and (5) oxidation of 1-naphthol. At this point, it is worth noting that the photosensitized oxidation of the majority of these probe compounds in homogeneous solution has been extensively investigated [65–71] and, as such, useful and reliable conclusions can be drawn. The heterogeneous photooxidation of the aforementioned compounds was carried out by using catalyst $C_{60}(3)$ or $C_{60}(6)$ and the findings are summarized in Table 4. The catalytic oxidations of entries 1–3 and 7–10 (Table 4) were carried out at 0 °C using 7.2 mg or 3.6 mg of $C_{60}(3)$ or $C_{60}(6)$ respectively (concentration of the active phase 3×10^{-4} M C_{60}) and 0.03 M of the organic substrate in 1 mL of CH_3CN . The catalytic oxidations of entries 4–6 (Table 4) were carried out at room temperature using 36 mg or 18 mg of $C_{60}(3)$ or $C_{60}(6)$ respectively (concentration of the active phase 3×10^{-4} M C_{60}) and 0.01 M of the organic substrate in 5 mL of the solvent. In all cases, the photooxidations of organic substrates 2–11 afforded the expected products 12–21. This observation clearly supports the intermediacy of 1O_2 in the C_{60} mediated heterogeneous photooxidations of 2–11.

It is worth mentioning that 2,3-dimethyl-2-butene (3, entry 2) was quantitatively converted to 3-hydroperoxy-2,3-dimethyl-1-butene (13) in 20 min, which is much shorter than the earlier

Table 4
Photooxidations of organic substrates **2–11** with catalyst C₆₀(3) or C₆₀(6).

Entry	Substrate	Product	Catalyst	Solvent	Reaction time	Conversion yield (%) ^a
1			C ₆₀ (6)	CH ₃ CN	3 h	45 ^b
2			C ₆₀ (6)	CH ₃ CN	20 min	>97 ^b
3			C ₆₀ (3)	CH ₃ CN	5 min	>97 ^d
4			C ₆₀ (3)	CH ₃ CN	12 h	>95 ^d
5			C ₆₀ (6)	CH ₃ CN	18 h	65 ^f
6			C ₆₀ (6)	<i>n</i> -Hexane ^g	17 h	>97 ^f
7			C ₆₀ (6)	CH ₃ CN	10 min	>97 ^b
8			C ₆₀ (6)	CH ₃ CN	10 min	>97 ^b
9			C ₆₀ (6)	CH ₃ CN	10 min	>97 ^b
10			C ₆₀ (6)	CH ₃ CN	30 min	92 ^b

^a The reported % conversion values are the average of three measurements obtained from three separate experiments.

^b Identified by GC and/or GC-MS spectroscopy. The reaction solution contained 5 μ L *n*-nonane as internal standard.

^c Ph₃P was added to the reaction mixture, in order to reduce the allylic hydroperoxides to the corresponding alcohols, and the resulting sample was left at room temperature for 20 min.

^d Identified using TLC and ¹H NMR spectroscopy.

^e The reaction mixture was chromatographed on silica gel (hexanes/EtOAc=9:1) to give endoperoxide **15** as a white solid in 84% overall yield. ¹H NMR (CDCl₃, 500 MHz) δ 7.54 (d, 4H, *J*=5 Hz), 7.46 (m, 6H), 6.38 (s, 2H), 5.73 (s, 2H) ppm; ¹³C NMR (125 MHz, CDCl₃) δ 137.7, 128.7, 128.6, 128.5, 127.4, 80.2 ppm.

^f Identified by GC and/or GC-MS spectroscopy.

^g The photooxidation of olefin **7** was carried out in *n*-hexane due to its insolubility in polar solvents, such as CH₃CN.

reported irradiation time [71–73]. Similarly, α -terpinene (**4**, entry 3) was quantitatively converted to the natural product ascaridole (**14**) after only 5 min. This photooxidation had been previously done: (1) with 90% yield after 30 min of irradiation using 0.5–1 mol% of C₆₀ [25], with 80% yield after 30 min of irradiation in the presence of azafullerenes C₅₉HN or (C₅₉N)₂ as sensitizers [74] and (3) with >97% yield after 1 h of irradiation using catalysts prepared by conjugating C₆₀ to amino-functional silica gels [73]. Moreover, diethyl sulfide (**8**, entry 7) was quantitatively oxidized to

diethyl sulfoxide (**18**) in 10 min, which is faster than the previously reported study [73]. Photooxidation of 1-naphthol (**11**, entry 10) afforded exclusively 1,4-naphthoquinone (**21**) in 92% conversion after only 30 min. Interestingly, the ¹O₂-mediated oxidation of this compound has been previously done: (1) with 90% yield after 10 h of irradiation with dissolved Methylene Blue [75], (2) with 64% yield after 35 min of irradiation using fullerene-coated polymer beads [71] and (3) with >97% yield after 90 min of irradiation using linked C₆₀ to amino-functionalized silica gels as catalysts [73]. Ultimately,

the above mentioned results provide strong evidence that the activity of the MCM-41 supported catalysts is much higher than that obtained for the unsupported C₆₀, azafullerenes C₅₉HN or (C₅₉N)₂, Methylene Blue, fullerene-coated polymer beads as well as linked C₆₀ to amino-functionalized silica gels.

4. Conclusions

Successive incipient wetness impregnation followed by heating at 180 °C is proved an efficient preparation method for dispersing effectively various amounts of C₆₀ (in the range 3–12 wt.%) on MCM-41 surface. The nature of the deposited species does not actually change upon impregnation or heating. The mesoporous structure of MCM-41 remains intact upon deposition of C₆₀ on its surface. The C₆₀ is highly dispersed within the mesopores or the external surface of MCM-41 as clusters or crystallites/aggregates of very small size. The mesopore size of all the photocatalyst remains similar to that of the support MCM-41, while a very small decrease (less than ca. 5%) is observed in the SSA and the total pore volume, especially in the highly loaded catalysts (with 9 and 12 wt.% C₆₀). A small reduction of the thermal stability of the supported C₆₀ has been found, compared to that of the bulk C₆₀, due to the very small size of the clusters or crystallites in the former case.

The activity of the heterogeneous photocatalysts was tested in the photooxidation of organic substrates via the ¹O₂ ene reaction, the [4 + 2] or [2 + 2] cycloaddition and the oxidation of phosphines, sulfides and phenols. These reactions were carried out at 0 °C or room temperature and atmospheric pressure, in the presence of molecular oxygen, by irradiation with visible light. Thus, these processes represent an environmentally benign synthetic route with potential applications in applied synthesis.

All catalysts proved to be very active exhibiting high conversion, turnover number and turnover frequency values compared to that of the unsupported (solid) C₆₀. This was attributed to the high dispersion of crystallites/aggregates of C₆₀ with very small size on the support surface. The photocatalyst with 6 wt.% C₆₀ presented the higher activity. The use of MCM-41 as a support instead of SiO₂ and γ-Al₂O₃, used in previous works, leads to photocatalysts with higher activity, attributed mainly to the higher dispersion of C₆₀ due to the high surface area of MCM-41. Shadow effects were not observed under our experimental conditions.

Acknowledgments

This work was supported by the Greek State Scholarships Foundation (I.K.Y.) through a postdoctoral research scholarship awarded to M.D.T. and M.N.A. The Foundation for Education and European Culture is also acknowledged for providing a one year fellowship to M.N.A.

References

- [1] P.R. Ogilby, *Chem. Soc. Rev.* 39 (2010) 3181–3209.
- [2] M.C. DeRosa, R.J. Crutchley, *Coord. Chem. Rev.* 233–234 (2002) 351–371.
- [3] E.L. Clennan, A. Pace, *Tetrahedron* 61 (2005) 6665–6691.
- [4] A.A. Frimer, *Singlet Oxygen*, in: A.A. Frimer (Ed.), CRC Press, Boca Raton, 1985.
- [5] T. Montagnon, M. Tofi, G. Vassilikogiannakis, *Acc. Chem. Res.* 41 (2008) 1001–1011.
- [6] J.F. Rabek, in: A.A. Frimer (Ed.), *Singlet Oxygen*, vol. 4, CRC Press, Boca Raton, 1985, pp. 1–90.
- [7] R.D. Scurlock, M. Kristiansen, P.R. Ogilby, V.L. Taylor, R.L. Clough, *Polym. Degrad. Stab.* 60 (1998) 145–159.
- [8] R.D. Scurlock, B. Wang, P.R. Ogilby, J.R. Sheats, R.L. Clough, *J. Am. Chem. Soc.* 117 (1995) 10194–10202.
- [9] E.S. Gonçalves, P.R. Ogilby, *Langmuir* 24 (2008) 9056–9065.
- [10] R.C. Straight, J.D. Spikes, in: A.A. Frimer (Ed.), *Singlet Oxygen*, vol. 4, CRC Press, Boca Raton, 1985, pp. 91–143.
- [11] R.W. Redmond, I.E. Kochevar, *Photochem. Photobiol.* 82 (5) (2006) 1178–1186.
- [12] M.J. Davies, *Biochem. Biophys. Res. Commun.* 305 (2003) 761–770.
- [13] M.T. Jarvi, M.J. Niedre, M.S. Patterson, B.C. Wilson, *Photochem. Photobiol.* 82 (2006) 1198–1210.
- [14] M. Prein, W. Adam, *Angew. Chem. Int. Ed. Engl.* 35 (1996) 477–494.
- [15] M. Stratakis, M. Orfanopoulos, *Tetrahedron* 56 (2000) 1595–1615.
- [16] C. Cantau, T. Pigot, N. Manoj, E. Oliveros, S. Lacomble, *Chem. Phys. Chem.* 8 (2007) 2344–2353.
- [17] N. Hoffmann, *Chem. Rev.* 108 (2008) 1052–1103.
- [18] G.O. Schenck, H. Eggert, W. Denk, *Liebigs Ann. Chem.* 584 (1953) 177–198.
- [19] M.N. Alberti, M. Orfanopoulos, *Synlett* 7 (2010) 999–1026.
- [20] M.N. Alberti, M. Orfanopoulos, *Chem. Eur. J.* 16 (2010) 9414–9421.
- [21] C. Schweitzer, R. Schmidt, *Chem. Rev.* 103 (2003) 1685–1757.
- [22] R. Schmidt, *Photochem. Photobiol.* 82 (2006) 1161–1177.
- [23] C.S. Foote, E.L. Clennan, in: C.S. Foote, J.S. Valentine, A. Greenberg, J.F. Liebman (Eds.), *Active Oxygen in Chemistry*, Chapman & Hall, London, 1995, pp. 105–140.
- [24] M. Orfanopoulos, S. Kambourakis, *Tetrahedron Lett.* 35 (1994) 1945–1948.
- [25] H. Tokuyama, E. Nakamura, *J. Org. Chem.* 59 (1994) 1135–1138.
- [26] M. Orfanopoulos, S. Kambourakis, *Tetrahedron Lett.* 36 (1995) 435–438.
- [27] J.W. Arbogast, A.P. Darmanyan, C.S. Foote, F.N. Diederich, R.L. Whetten, Y. Rubin, M.M. Alvarez, S.J. Anz, *J. Phys. Chem.* 95 (1991) 11–12.
- [28] M. Terazima, N. Hirota, H. Shinohara, Y. Saito, *J. Phys. Chem.* 95 (1991) 9080–9085.
- [29] M.R. Fraelich, R.B. Weisman, *J. Phys. Chem.* 97 (1993) 11145–11147.
- [30] Y. Kajii, T. Nakagawa, S. Suzuki, Y. Achiba, K. Obi, K. Shibuya, *Chem. Phys. Lett.* 181 (1991) 100–104.
- [31] P.J. Krusic, E. Wasserman, B.A. Parkinson, B. Malone, E.R. Holler Jr., P.N. Keizer, J.R. Morton, K.F. Preston, *J. Am. Chem. Soc.* 113 (1991) 6274–6275.
- [32] J.W. Arbogast, C.S. Foote, M. Kao, *J. Am. Chem. Soc.* 114 (1992) 2277–2279.
- [33] M.D. Tzirakis, M. Orfanopoulos, *Org. Lett.* 10 (2008) 873–876.
- [34] M.D. Tzirakis, M. Orfanopoulos, *J. Am. Chem. Soc.* 131 (2009) 4063–4069.
- [35] M.D. Tzirakis, M.N. Alberti, M. Orfanopoulos, *Chem. Commun.* 46 (2010) 8228–8230.
- [36] M.D. Tzirakis, M. Orfanopoulos, *Angew. Chem. Int. Ed.* 49 (2010) 5891–5893.
- [37] M.D. Tzirakis, M.N. Alberti, M. Orfanopoulos, *Org. Lett.* 13 (2011) 3364–3367.
- [38] M.D. Tzirakis, J. Vakros, L. Loukatzikou, V. Amargianitakis, M. Orfanopoulos, C. Kordulis, A. Lycourghiotis, *J. Mol. Catal. A-Chem.* 316 (2010) 65–74.
- [39] G.D. Panagiotou, M.D. Tzirakis, J. Vakros, L. Loukatzikou, M. Orfanopoulos, C. Kordulis, A. Lycourghiotis, *Appl. Catal. A-Gen.* 372 (2010) 16–25.
- [40] C.T. Kresge, M.E. Leonowicz, W.J. Roth, J.C. Vartuli, J.S. Beck, *Nature* 359 (1992) 710–712.
- [41] A. Monnier, F. Schüth, Q. Huo, D. Kumar, D. Margolese, R.S. Maxwell, G.D. Stucky, M. Krishnamurty, P. Petroff, A. Firouzi, M. Janicke, B.F. Chmelka, *Science* 261 (1993) 1299–1303.
- [42] J.S. Beck, J.C. Vartuli, W.J. Roth, M.E. Leonowicz, C.T. Kresge, K.D.C. Schmitt, T.-W. Chu, D.H. Olson, E.W. Sheppard, S.B. McCullen, J.B. Higgins, J.L. Schlenker, *J. Am. Chem. Soc.* 114 (1992) 10834–10843.
- [43] S. Rodrigues, K.T. Ranjit, S. Uma, I.N. Martyanov, K.J. Klabunde, *J. Catal.* 230 (2005) 158–165.
- [44] Y. Hu, N. Wada, K. Tsujimaru, M. Anpo, *Catal. Today* 120 (2007) 139–144.
- [45] S. Rodrigues, S. Uma, I.N. Martyanov, K.J. Klabunde, *J. Catal.* 233 (2005) 405–410.
- [46] A. Maldotti, A. Molinari, G. Varani, M. Lenarda, L. Storaro, F. Bigi, R. Maggi, A. Mazzacani, G. Sartori, *J. Catal.* 209 (2002) 210–216.
- [47] Y. Shiraishi, H. Ohara, T. Hirai, *J. Catal.* 254 (2008) 365–373.
- [48] Y. Guo, C. Hua, *J. Mol. Catal. A: Chem.* 262 (2007) 136–148.
- [49] M.J. Verhoef, P.J. Kooyman, J.A. Peters, H. van Bekkum, *Micropor. Mesopor. Mater.* 27 (1999) 365–371.
- [50] H. Yoshida, T. Shimizu, C. Murata, T. Hattori, *J. Catal.* 220 (2003) 226–232.
- [51] A. Maldotti, A. Maldotti, A. Bratovic, G. Magnacca, *Catal. Today* 161 (2011) 64–69.
- [52] M. Grün, K.K. Unger, A. Matsumoto, K. Tsutsumi, *Micropor. Mesopor. Mat.* 27 (1999) 207–216.
- [53] A.P. Fotopoulos, K.S. Triantafyllidis, *Catal. Today* 127 (2007) 148–156.
- [54] M.N. Alberti, M. Orfanopoulos, *Org. Lett.* 10 (2008) 2465–2468.
- [55] A.B. Smith, H. Tokuyama, R.M. Strongin, G.T. Furst, W.J. Romanow, B.T. Chait, U.A. Mirza, I. Haller, *J. Am. Chem. Soc.* 117 (1995) 9359–9360.
- [56] K.M. Creagan, J.L. Robbins, W.K. Robbins, J.M. Millar, R.D. Sherwood, P.J. Tindall, D.M. Kox, A.M. Smith, J.P. McCauley Jr., D.R. Jones, R.T. Gallagher, *J. Am. Chem. Soc.* 114 (1992) 1103–1105.
- [57] E. Ntararas, H. Matralis, G.M. Tsigoulis, *Tetrahedron Lett.* 45 (2004) 4389–4391.
- [58] R.S. Ruoff, D.S. Tse, R. Malhotra, D.C. Lorents, *J. Phys. Chem.* 97 (1993) 3379–3383.
- [59] K.N. Semenov, N.A. Charykov, V.A. Keskinov, A.K. Piartman, A.A. Blokhin, A.A. Kopyrin, *J. Chem. Eng. Data* 55 (2010) 13–36.
- [60] M.R. Ilesce, in: A.G. Griesbeck, J. Mattay (Eds.), *Synthetic Organic Photochemistry*, 11, Marcel Dekker, New York, 2005, pp. 299–363.
- [61] W. Adam, A.G. Griesbeck, in: W.M. Horspool, P.-S. Song (Eds.), *CRC Handbook of Organic Photochemistry and Photobiology*, CRC Press, Boca Raton, 1995, pp. 311–324.
- [62] W. Adam, M. Prein, *Acc. Chem. Res.* 29 (1996) 275–283.
- [63] A.L. Baumstark, A. Rodriguez, in: W.M. Horspool, P.-S. Song (Eds.), *CRC Handbook of Organic Photochemistry and Photobiology*, CRC Press, Boca Raton, 1995, pp. 335–345.
- [64] A. Gorman, in: D.H. Volman, G.S. Hammond, D.C. Neckers (Eds.), *Advances in Photochemistry*, 17, Wiley, New York, 1992, pp. 217–274.
- [65] K. Gollnick, G.O. Schenck, *Pure Appl. Chem.* 9 (1964) 507–525.

- [66] G.O. Schenck, K. Schulte-Elte, *Liebigs Ann. Chem.* 618 (1958) 185–193.
- [67] G.O. Schenck, *Angew. Chem.* 69 (1957) 579–599.
- [68] G. Rio, J. Berthelot, *Bull. Soc. Chem. Fr.* 5 (1969) 1664–1667.
- [69] Y. Cao, B.W.Y.F. Zhang, Ming J.X. Chen, *J. Photochem.* 38 (1987) 131–144.
- [70] S. Tsuji, M. Kondo, K. Ishiguro, Y. Sawaki, *J. Org. Chem.* 58 (1993) 5055–5059.
- [71] A.W. Jensen, C. Daniels, *J. Org. Chem.* 68 (2003) 207–210.
- [72] E.C. Blossey, D.C. Neckers, A.L. Thayer, A.P. Schaap, *J. Am. Chem. Soc.* 95 (1973) 5820–5822.
- [73] T. Hino, T. Anzai, N. Kuramoto, *Tetrahedron Lett.* 47 (2006) 1429–1432.
- [74] N. Tagmatarchis, H. Shinohara, *Org. Lett.* 2 (2000) 3551–3554.
- [75] H.M. Chawla, K. Kaul, M. Kaul, *Indian J. Chem. Sect. B* 32 (1993) 733–737.